

Published in final edited form as:

Nat Ecol Evol. 2018 June ; 2(6): 1019–1024. doi:10.1038/s41559-018-0542-2.

Native iron reduces CO₂ to intermediates and end-products of the acetyl CoA pathway

Sreejith J. Varma[#], Kamila B. Muchowska[#], Paul Chatelain, and Joseph Moran^{*}

Institute of Supramolecular Science and Engineering (ISIS UMR 7006), University of Strasbourg, National Center for Scientific Research (CNRS), F-67000 Strasbourg, France

[#] These authors contributed equally to this work.

Abstract

Autotrophic theories for the origin of life propose that CO₂ was the carbon source for primordial biosynthesis. Among the six known CO₂ fixation pathways in nature, the acetyl CoA (or Wood-Ljungdahl) pathway is the most ancient, and relies on transition metals for catalysis. Modern microbes that use the acetyl CoA pathway typically fix CO₂ with electrons from H₂, which requires complex flavin-based electron bifurcation. This presents a paradox: How could primitive metabolic systems have fixed CO₂ before the origin of proteins? Here we show that native transition metals (Fe⁰, Ni⁰, Co⁰) selectively reduce CO₂ to acetate and pyruvate, the intermediates and end-products of the AcCoA pathway, in near mM levels in water over hours to days using 1–40 bar CO₂ and at temperatures from 30–100 °C. Geochemical CO₂ fixation from native metals could have supplied critical C2 and C3 metabolites before the emergence of enzymes.

From the very earliest stages of the transition from chemistry to biochemistry at the origin of life, synthetic pathways must have operated to build molecular complexity from simple starting materials. Life's fundamental need to build up carbon-based molecules has understandably oriented research on prebiotic chemistry towards high energy C1 and C2 compounds such as HCN and formaldehyde, which react in ways that bear little resemblance to biosynthesis, often requiring UV light.^{1,2,3} However, as far as we can infer from extant biology, life has always built its biomass from CO₂. Could this attribute have extended back to prebiotic chemistry? Of the six known pathways of CO₂ fixation in nature,^{4,5} the acetyl CoA (or Wood-Ljungdahl) pathway is the most ancient.^{6,7,8} It reduces CO₂ to acetyl and then to pyruvate, the ubiquitous C2 and C3 building blocks for life. Its enzymes and co-factors are replete with transition metals (Fe, Ni, Co, Mo or W) and unlike the other five

Users may view, print, copy, and download text and data-mine the content in such documents, for the purposes of academic research, subject always to the full Conditions of use:http://www.nature.com/authors/editorial_policies/license.html#terms

moran@unistra.fr.

Data availability.

The data that support the findings of this study are available in the Supplementary Information.

Author contributions

J.M. supervised the research and the other authors performed the experiments. All authors contributed intellectually throughout the study. J.M. and K.B.M wrote the paper and S.J.V. and K.B.M. assembled the Supplementary Information. Important preliminary experiments were carried out by P.C.

Competing Interests

The authors declare no competing interests.

pathways, it is short, linear, exergonic and found in both bacteria and archaea, with the archaeal version being ATP-independent (Fig. 1).^{9,10,11,12} For all these reasons, the acetyl CoA pathway is often proposed to have prebiotic origins,¹³ though such a proposition faces some difficulties. Most modern microbes that run the acetyl CoA pathway fix CO₂ using electrons from H₂ gas, whose midpoint potential is not sufficient to generate the required highly reduced ferredoxin proteins in the absence of flavin-based electron bifurcation.¹⁴ Therein lies a problem for autotrophic theories of the origin of life: How could CO₂ fixation have occurred before there were proteins to enable electron bifurcation? Many experimental attempts to address this question have bypassed the direct use of CO₂ altogether, focusing instead on its more reduced derivatives such as CO or formic acid.^{15,16} However, clues from extant biology and the chemical literature suggest that native metals might warrant further experimental consideration as a prebiotic source of electrons for CO₂ fixation.¹⁷ Even today, some bacteria that use the acetyl CoA pathway grow using native iron as the sole source of electrons.^{18,19} We recently reported chemical experiments where many reactions of the rTCA cycle, another potentially prebiotic CO₂-fixing pathway, can be driven in sequence without enzymes using native iron as the source of electrons.²⁰ Meanwhile, freshly prepared native iron nanoparticles have been shown to reduce CO₂ to formate, with acetate formed as a minor product at 200 °C under 40 bar CO₂ pressure.²¹ Before the emergence of electron bifurcating enzymes, could native metals achieve reductive CO₂ fixation under conditions mild enough for a protometabolism?

Results and discussion

Anticipating a link between the role of metallic cofactors in extant microbial metabolism and in prebiotic chemistry,^{22,23,24} we set out to investigate whether the native forms of the metals involved in the reductive AcCoA pathway might promote C-C bond formation from CO₂ in water. We initially screened reactions of 1 mmol of Fe, Co, Ni, Mn, Mo and W powders (for specifications see Supplementary Table 1) in a 1 M KCl solution in deionized H₂O by heating to 100 °C under 35 bar CO₂ pressure for 16 h. The reaction mixtures were then treated with KOH to precipitate hydroxides, which were removed by centrifugation prior to analysis by ¹H NMR and GC-MS (Supplementary Figs. 1 – 8). Quantification was achieved by comparison to a calibration curve prepared from authentic samples (Supplementary Fig. 9). To our surprise, all of these metals were found to promote the formation of acetate in up to 0.28 ± 0.01 mM concentration, with considerable amounts of pyruvate observed in the cases of iron (0.03 ± 0.01 mM), nickel (0.02 ± 0.00 mM) and cobalt (0.01 ± 0.00 mM) (Fig. 2). Substantial quantities of formate (up to 2.3 ± 0.2 mM in the case of cobalt) and methanol (up to 0.39 ± 0.00 mM in the case of molybdenum) were also found in almost all cases. Control experiments in the absence of metal powders or in the absence of CO₂ did not produce detectable quantities of carbon fixation products (Supplementary Figs. 10 and 11).

In light of iron's position as the premier Earth-abundant metal (predominantly as Fe⁰ in the Earth's core and as Fe²⁺/Fe³⁺ in the Earth's mantle and crust)²⁵, we elected to study iron-mediated CO₂ fixation in more detail by evaluating the influence of temperature, pressure, time, pH, salt identity and salt concentration on the reaction outcome. First, we studied the effect of temperature over the range 30-150 °C under typical conditions (35 bar CO₂,

unbuffered 1 M KCl solution in deionized H₂O, 16 h) (Fig. 3a, see also Supplementary Figs. 12 and Supplementary Table 2). At the lower end of the temperature range, acetate is the major product in solution, with pyruvate and formate formed in slightly smaller quantities. Increasing the reaction temperature to 100 °C results in the appearance of methanol among the other products. At 150 °C, pyruvate is no longer observed, presumably due to thermal decomposition. The reaction is robust to CO₂ pressure over the investigated range 1-40 atm at 30 °C, with acetate and pyruvate being the major products at lower pressures (Fig. 3b, see also Supplementary Fig. 13 and Supplementary Table 3). The reaction progress was monitored at different times under two representative sets of conditions. At 30 °C and 1 bar CO₂ acetate and pyruvate are the major products, with the former reaching nearly 0.7 mM after 40 h before decreasing in concentration (Fig. 3c). At 100 °C and 35 bar CO₂ the initial buildup of formate is rapid, increasing to 7.2 ± 0.4 mM after 6 h before decreasing sharply as acetate and pyruvate begin to appear (Fig. 3d, see also Supplementary Fig. 14 and Supplementary Table 4). After 60 h, acetate and pyruvate reach maximal concentrations of 1.09 ± 0.00 mM and 0.11 ± 0.01 mM, respectively. Stopping the reaction at this time reveals that no Fe⁰ visibly remains, though only $\approx 1\%$ of the available electrons from Fe⁰ were channeled towards the described C1-C3 products in solution (assuming Fe²⁺ is the terminal product, see Supplementary Table 5), supporting previous observations that Fe⁰ predominantly reacts to form hydrogen under these conditions.²⁶ By 85 h, the concentrations of all products in solution decrease, and ethanol is detected in the reaction mixtures for the first time (Supplementary Fig. 15). The disappearance of the Fe⁰ “fuel” necessary to maintain the reaction in a steady state presumably causes the thermal decomposition of C2 and C3 products to outcompete their generation.²⁷ Neither changing the initial unbuffered pH nor swapping the K⁺ electrolyte for other biologically relevant inorganic cations (Na⁺, Mg²⁺ and Ca²⁺) had significant influence on carbon fixation (Supplementary Figs. 16 – 26 and Supplementary Tables 6 – 17). However, the salt concentration had a small but significant effect, with a drop of acetate and pyruvate yields by over 20% in the absence of KCl (Supplementary Fig. 27 and Supplementary Table 18).

Several additional experimental observations helped to gain insight into the mechanism of the reaction. First, in the absence of basic workup with KOH prior to NMR analysis, no C1 – C3 carbon fixation products were observed in solution (Supplementary Fig. 29). Second, introduction of formate, methanol or acetate into the reactor under typical reaction conditions did not result in their conversion to higher C2 or C3 products (Supplementary Fig. 30). Thus, formate, methanol and acetate, free in solution, do not appear to be intermediates in the reaction. Third, lactate, the product of pyruvate reduction, was never observed in any of our experiments, despite the fact that it is readily detected upon exposure of an aqueous pyruvate solution to native Fe (Supplementary Fig. 30d). Fourth, Fe-mediated carbon fixation reactions performed with CO instead of CO₂ at 100 °C produced only tiny amounts of acetate and no detected pyruvate (Supplementary Fig. 31 and Supplementary Table 19). On the basis of these observations, we conclude that CO₂ fixation occurs on the surface of the metal and that its intermediates and end-products remain bound to the surface during the reaction. In light of this surface chemistry, the observed product distribution and the reaction’s kinetic profile, we propose a plausible yet still largely hypothetical mechanism whereby initial reduction of CO₂ occurs to generate surface-bound carbon monoxide and

formyl groups. Further reductions of the formyl group with expulsion of water leads to a surface-bound methyl group. Chain growth via migratory insertion of carbon monoxide into the methyl group produces an acetyl species, which itself can undergo further migratory insertion of CO or reductive carboxylation with CO₂ to furnish a surface-bound pyruvyl or pyruvate species, respectively. The resistance of pyruvate or pyruvyl to reduction by Fe⁰ may be rationalized by a diminished reactivity of the surface-bound species compared to pyruvate in solution. Basic workup at the end of the reaction with KOH is required to cleave the products from the surface to furnish formate, methanol, acetate or pyruvate in solution (Fig. 4). One possible interpretation of the kinetic profile observed in Fig. 3c is that the Fe surface becomes initially saturated with formyl and CO groups, with subsequent reactions of those groups producing acetyl and, eventually, pyruvyl groups.²⁴ Further detailed mechanistic study is required to distinguish between the possible intermediacy of surface-bound metal carboxylates and surface acyl metal species.

Besides the acetyl CoA pathway, another carbon fixation pathway that is often proposed to be ancient is the reductive tricarboxylic acid cycle²⁸ (rTCA cycle; also known as the reverse Krebs cycle, reductive citric acid cycle or the Arnon-Buchanan cycle; see Fig. 5), which contains five metabolites that collectively serve as the universal biosynthetic precursors for all of biochemistry.^{29,30,31,32} A shorter, linear form of the rTCA cycle incorporating the first six steps (steps A-F), known as the “horseshoe”, also contains the same five crucial metabolites. We recently demonstrated that the combination of Fe⁰, Zn²⁺ and Cr³⁺ under strongly acidic conditions (1 M HCl in H₂O) promotes six of the eleven steps of the rTCA cycle in the absence of enzymes, including the oxaloacetate-to-succinate sequence (steps C-E) and the oxalosuccinate-to-citrate sequence (steps H-J).²⁰ Since they share a common step (step A), it has been proposed that either the complete or “horseshoe” forms of the rTCA cycle may have once been united with the acetyl CoA pathway in an ancestral, possibly prebiotic, carbon fixation network.^{13,24,33,34} While these proposals provide strong explanatory power for the structure of extant metabolism, supporting chemical evidence is critically lacking. In light of the functional similarities between the CO₂ fixation reactions described in the current work and the acetyl CoA pathway, as well as the reliance of both chemistries on native iron, experiments were conducted to assess the mutual compatibility of the newly uncovered carbon fixation reaction with non-enzymatic reactions of the rTCA cycle. When oxaloacetate was heated for 16 h in the presence of Fe powder and Cr³⁺ at 140 °C under 35 bar of CO₂, an appreciable amount of succinate was formed, as evidenced by NMR and GC-MS (Supplementary Figs. 32 and 33). An analogous experiment carried out with *in situ* generated oxalosuccinate (heated at 140 °C for 16 h under 35 bar of CO₂, in the presence of Fe powder and Cr³⁺) resulted in the formation of citrate (detected by GC-MS, Supplementary Fig. 34). Although both of these reaction sequences are less selective under the mildly acidic conditions afforded by CO₂-saturated water than in 1 M HCl, they nonetheless suggest the potential compatibility of the carbon fixation conditions shown here with the non-enzymatic promotion of rTCA cycle reaction sequences. Lastly, the introduction of hydrazine into the otherwise identical Fe-rich conditions allowed for the non-enzymatic synthesis of the amino acid alanine from pyruvate (Supplementary Fig. 35).²⁰

Conclusions

We have shown that zero-valent forms of metals used by the cofactors and metalloenzymes of the AcCoA pathway fix CO₂ to selectively furnish the intermediates and end-products of that pathway in the absence of enzymes and in a manner robust to changes in temperature, pressure, salts and pH. Acetate is produced as the major C₂ product for all metals studied, whereas Fe⁰, Ni⁰ and Co⁰ also produce pyruvate in up to ~0.1 mM concentrations, demonstrating that non-enzymatic C-C bond-formation from CO₂ is possible in water under exceptionally mild conditions. The high selectivity of Fe⁰ for the critical metabolites acetate and pyruvate at 30 °C and 1 atm CO₂ is remarkable considering the large number of C₂ and C₃ compounds derived from C, H and O that could possibly have been produced, suggesting that these compounds represent kinetic paths of least resistance for reductive organic synthesis from CO₂. Control and time course experiments support a mechanism where CO₂ fixation occurs on the surface to produce surface-bound intermediates, notably reminiscent of some aspects of Wächtershäuser's initial theory of surface metabolism.²⁹ The temperature dependence and critical need to liberate surface-bound species with KOH prior to analysis may explain why pyruvate was not observed in previous studies on the reaction of CO₂ with Fe⁰.^{21,26} The CO₂ fixation reactions reported here are more geochemically plausible than the synthesis of activated acetate from CO and CH₃SH,^{15,35} the low yielding and non-selective synthesis of pyruvate (0.07%) in formic acid at high temperature and high pressure (250 °C, 2000 bar),¹⁶ or using highly reducing (-1.1 V) electrochemistry on greigite electrodes.³⁶ Although native telluric iron deposits in the modern Earth's crust are relatively rare,³⁷ native iron is produced in small amounts during serpentinization in the form of reduced FeNi minerals whose presence in surface samples indicates that they oxidize quite slowly.^{38,39} Native iron is produced transiently in the mantle,⁴⁰ and is the major component of the Earth's core. Iron meteorites, which constitute nearly 90% of known meteoritic mass, are mostly composed of native iron and its various alloys with nickel.^{41,42} Thus, numerous plausible geological scenarios might be imagined in which Fe⁰ or other reduced metals could have been continuously produced and consumed on the early Earth, in general agreement with the idea that metabolism originated to relieve pent-up redox gradients between the reduced iron that formed the early Earth's bulk and its comparatively oxidized CO₂-rich atmosphere and oceans,⁴³ a concept referred to as geobiotropy.^{44,45} It may also help explain why pyruvate is found in some meteorites.⁴⁶ The Fe⁰-promoted carbon fixation conditions are mutually compatible with Fe⁰-promoted non-enzymatic transformations of other supposedly ancient metabolic pathways, describing a set of reactions that play a synthetic role equivalent to the reductive AcCoA pathway, up to 7 of the 11 reactions of the rTCA cycle and amino acid synthesis. The observation that surface-bound pyruvate is not reduced to lactate in the presence of Fe⁰ - though not yet fully understood - opens up new mechanistic possibilities for how non-enzymatic anabolic reactions might be promoted selectively in the face of potential parasitic reactions.⁴⁷ The observed reactivity demonstrates a significant parallel between plausible prebiotic chemistry and the ancient CO₂-fixing pathways used by primitive autotrophic life, supporting the hypothesis that geochemistry could have played an important role in the origin of life.

Methods

Analytical methods

¹H NMR spectra were recorded on a Bruker Avance300 (300 MHz) spectrometer at ambient temperature in a 6:1 H₂O:D₂O mixture as solvent, with sodium 3-(trimethylsilyl)-1-propanesulfonate (DSS-Na) as the internal standard (CH₃ peak at 0 ppm). Solvent suppression was achieved through excitation sculpting, using the Bruker ZGESGP pulse program adjusted for the water resonance. 32 scans were acquired for each sample. Relaxation delay D1 was set to 87 s, with time domain size TD = 32768 and sweep width SWH = 4789.27 Hz (11.963 ppm), to allow for quantitative measurements. Integration was performed using *MestReNova v6.0.2* software. Gas chromatography-mass spectrometry analysis was performed on a GC System 7820A (G4320) using an Agilent High Resolution Gas Chromatography Column (PN 19091S – 433UI, HP – 5MS UI, 28 m×0.250 mm, 0.25 Micron, SN USD 489634H). The system was connected to an MSD block 5977E (G7036A). Hydrogen (99.999 % purity) was used as carrier gas at a constant flow rate of 1.5 mL min⁻¹. The analysis was carried out in a splitless mode with 1 μL injection volume, at the injection port temperature of 250 °C. The column was maintained at 60 °C for 1 min, then ramped at 30 °C min⁻¹ to 310 °C with 3 min hold, and the total running time was 12.33 min. The mass spectrometer was turned on after a 2-min solvent delay and was operated at the electron ionization (EI) mode with quadrupole temperature of 150 °C. Data was acquired in the full-scan mode (50-500 amu).

Product Identification

Acetate, pyruvate, methanol, formate and lactate were identified based on the chemical shifts in the ¹H NMR, compared to authentic samples using sodium 3-(trimethylsilyl)-1-propanesulfonate (DSS-Na) as the internal standard. Formate, acetate and pyruvate were additionally confirmed by GC-MS, where they were detected as their amides derived from *N*-methylphenylethylamine. Pyruvate was additionally confirmed by GC-MS. Pyruvate in the post-treatment sample was first reduced to lactate and converted to its ethyl ester (see below), since lactate esters have a better response than pyruvate esters.²⁰ See the Supplementary Information for more details regarding these procedures.

NMR sample preparation

To the reaction mixture was added ~300 mg of solid KOH (NaHS·xH₂O in the case of Mo-promoted reactions) in order to precipitate out any metal ions as their hydroxides (or sulfides in the case of Mo). This was mixed thoroughly. The resulting thick suspension was transferred to a 1.5 mL plastic microtube and centrifuged at 10 000 rpm for 20 minutes. To 600 μL of the supernatant was added 100 μL of 0.05 M solution of internal standard (DSS-Na in D₂O). The resulting solution was analysed by NMR using the Bruker ZGESGP pulse program.

Yield determination and error analysis

700 μL aqueous solutions of potassium acetate, sodium methoxide, sodium pyruvate and sodium formate at different concentrations (0.71, 1.78, 3.57, 5.35, 7.14, 8.92 and 10.71 mM)

were prepared by diluting their respective stock solutions (50 mM in Milli-Q water) with Milli-Q water to 600 μ L and adding to each an aliquot of 100 μ L of 50 mM solution of the standard compound (DSS-Na) in D₂O. Each of the samples was prepared in two replicas by two researchers and subjected to NMR spectroscopy (¹H, ZGESGP water suppression, as described above). For each of these, three 32-scan spectra were acquired. The data from these six measurements for every concentration allowed us to obtain seven-point calibration plots for formate, methanol, acetate and pyruvate, correlating the substrate-to-standard ratios of peaks (8.45 ppm for formate, 3.34 ppm for methanol, 2.36 for pyruvate or 2.08 ppm for acetate, 0 ppm for the methyl peak of the standard DSS-Na) with the product concentration (See Supplementary Fig. 9). The data points were subjected to least-squares fitting (intercept = 0), from which the calibration line equation was obtained. Detection thresholds were estimated for each analyzed compound by integrating across the baseline in these regions of NMR spectra where no peaks were present, and were thus established to be 0.007 mM for acetate and pyruvate, 0.0016 mM for formate and 0.0026 mM for methanol. We note these values are much below the concentrations of acetate, pyruvate, methanol and formate detected in this study (See Supplementary Tables 2 – 19). Error bars on the calibration graphs correspond to \pm standard deviation for each data point. The yields of the CO₂ fixation experiments were calculated using the calibration coefficient corresponding to the slope of each calibration line. All yields of the CO₂ fixation experiments reported in this study are an average of at least two independent runs, with an error corresponding to \pm mean absolute deviation (see Supplementary Information).

Metal-promoted CO₂ fixing reactions

To a 1.5 mL glass vial with a PTFE-coated stir-bar was added 1 mmol of each tested reagent (56 mg Fe, or 58 mg Co, or 58 mg Ni, or 55 mg Mn, or 96 mg Mo, or 184 mg W, and/or 58 mg NaCl, and/or 75 mg KCl, and/or 95 mg MgCl₂, and/or 111 mg CaCl₂) and 1 mL of Milli-Q water. To prevent cross-contamination, the vials were closed with caps bearing punctured PTFE septa. After placing the vials in a stainless-steel 300 mL Parr pressure reactor, it was flushed with *ca.* 5 bar CO₂, pressurized to a final value of 35 bar CO₂ (unless noted otherwise), and stirred at the desired temperature (an external heating mantle was used where needed) for 16 h.

Assessment of compatibility of metal-promoted CO₂ fixation with rTCA cycle sequences

To a 1.5 mL glass vial with a PTFE-coated stir-bar were added carboxylic acid substrate (oxaloacetic acid (0.03 mmol, 4 mg) or triethyl oxalosuccinate (0.03 mmol, \sim 8 μ L)), Fe⁰ powder (1.0 mmol, 56 mg), KCl (1.0 mmol, 75 mg) and Cr₂(SO₄)₃·12H₂O (1 equiv., 0.030 mmol, 18 mg). This was followed by the addition of 1.0 mL of 0.24 M HCl in H₂O (2.0 μ L conc. HCl in 1.0 mL MilliQ H₂O), which corresponds to an initial pH = \sim 0.6. To prevent cross-contamination, the vial was closed with a cap with a punctured PTFE septum. After placing the vial in a stainless-steel 300 mL Parr pressure reactor, it was flushed with *ca.* 5 bar CO₂, pressurized to a final value of 35 bar CO₂, and stirred at 140 °C (an external heating mantle was used) for 16 h.

Procedure for reductive amination under conditions for metal-promoted CO₂ fixation

To a 1.5-mL glass vial with a PTFE-coated stir-bar was added sodium pyruvate (1 equiv, 0.03 mmol, 3 mg) in 1 mL MilliQ H₂O, hydrazine monohydrate (2 equiv, 0.06 mmol, ~3 μ L), KCl (1.0 mmol, 75 mg), followed by Fe⁰ powder (1.0 mmol, 56 mg). To prevent cross-contamination, the vial was closed with a cap with a punctured PTFE septum. After placing the vial in a stainless-steel 300 mL Parr pressure reactor, it was flushed with *ca.* 5 bar CO₂, pressurized to a final value 35 bar CO₂, and stirred at 140 °C (an external heating mantle was used) for 16 h.

Supplementary Material

Refer to Web version on PubMed Central for supplementary material.

Acknowledgments

This project has received funding from the European Research Council (ERC) under the European Union's Horizon 2020 research and innovation program (grant agreement n° 639170). Further funding was provided by a grant from LabEx "Chemistry of Complex Systems". L. Allouche, M. Coppe and B. Vincent are gratefully acknowledged for their assistance with NMR experiments. We thank E. Smith and W. F. Martin for critical readings of this manuscript.

References

1. Ruiz-Mirazo K, Briones C, de la Escosura A. Prebiotic systems chemistry: new perspectives for the origins of life. *Chem Rev.* 2014; 114:285–366. and references therein. [PubMed: 24171674]
2. Peretó J. Out of fuzzy chemistry: from prebiotic chemistry to metabolic networks. *Chem Soc Rev.* 2012; 41:5394–5403. [PubMed: 22508108]
3. Sutherland JD. Studies on the origin of life - the end of the beginning. *Nat Rev Chem.* 2017; 1:1.
4. Berg, et al. Autotrophic carbon fixation in archaea. *Nat Rev Microbiol.* 2010; 8:447–460. [PubMed: 20453874]
5. Hügl M, Sievert SM. Beyond the Calvin cycle: autotrophic carbon fixation in the ocean. *Annu Rev Mar Sci.* 2011; 3:261–289.
6. Ljungdahl LG, Irion E, Wood HG. Total synthesis of acetate from CO₂. I. Co-methylcobyrinic acid and co-(methyl)-5-methoxy-benzimidizolycobamide as intermediates with *Clostridium thermoaceticum*. *Biochemistry.* 1965; 4:2771–2779. [PubMed: 5880685]
7. Fuchs G. Alternative pathways of carbon dioxide fixation: insights into the early evolution of life? *Annu Rev Microbiol.* 2011; 65:631–658. [PubMed: 21740227]
8. Weiss MC, et al. The physiology and habitat of the last universal common ancestor. *Nat Microbiol.* 2016; 1 16116.
9. Can M, Armstrong FA, Ragsdale SW. Structure, function, and mechanism of the nickel metalloenzymes, CO dehydrogenase and acetyl-CoA synthase. *Chem Rev.* 2014; 114:4149–4174. [PubMed: 24521136]
10. Schwarz G, Mendel RR, Ribbe MW. Molybdenum cofactors, enzymes and pathways. *Nature.* 2009; 460:839–847. [PubMed: 19675644]
11. Schuchmann K, Müller V. Autotrophy at the thermodynamic limit of life: a model for energy conservation in acetogenic bacteria. *Nat Rev Microbiol.* 2014; 12:809–821. [PubMed: 25383604]
12. Furdui C, Ragsdale SW. The role of pyruvate ferredoxin oxidoreductase in pyruvate synthesis during autotrophic growth by the Wood-Ljungdahl pathway. *J Biol Chem.* 2000; 275:28494–28499. [PubMed: 10878009]
13. Martin W, Russell MJ. On the origin of biochemistry at an alkaline hydrothermal vent. *Phil Trans R Soc B.* 2007; 362:1887–1926. [PubMed: 17255002]

14. Herrmann G, Jayamani E, Mai G, Buckel W. Energy conservation via electron-transferring flavoprotein in anaerobic bacteria. *J Bacteriol.* 2008; 190:784–791. [PubMed: 18039764]
15. Huber C, Wächtershauser G. Activated acetic acid by carbon fixation on (Fe,Ni)S under primordial conditions. *Science.* 1997; 276:245–247. [PubMed: 9092471]
16. Cody GD, et al. Primordial carbonylated iron-sulfur compounds and the synthesis of pyruvate. *Science.* 2000; 289:1337–1340. [PubMed: 10958777]
17. Sousa FL, Preiner M, Martin WF. Native metals, electron bifurcation, and CO₂ reduction in early biochemical evolution. *Curr Opin Microbiol.* 2018; 43:77–83. [PubMed: 29316496]
18. Kato S, Yumoto I, Kamagata Y. Isolation of acetogenic bacteria that induce biocorrosion by utilizing metallic iron as the sole electron donor. *Appl Env Microbiol.* 2015; 81:67–73. [PubMed: 25304512]
19. Daniels L, Belay N, Rajagopal BS, Weimer PJ. Bacterial methanogenesis and growth from CO₂ with elemental Iron as the sole source of electrons. *Science.* 1987; 237:509–511. [PubMed: 17730323]
20. Muchowska K, et al. Metals promote sequences of the reverse Krebs cycle. *Nat Ecol Evol.* 2017; 1:1716–1721. [PubMed: 28970480]
21. He C, Tian G, Liu Z, Feng S. A mild hydrothermal route to fix carbon dioxide to simple carboxylic acids. *Org Lett.* 2010; 12:649–651. [PubMed: 20104858]
22. Sousa F, Martin WF. Biochemical fossils of the ancient transition from geoeconomics to bioenergetics in prokaryotic one carbon metabolism. *Biochim Biophys Acta.* 2014; 1837:964–981. [PubMed: 24513196]
23. Morowitz HJ, Srinivasan V, Smith E. Ligand field theory and the origin of life as an emergent feature of the periodic table of elements. *Biol Bull.* 2010; 219:1–6. [PubMed: 20813983]
24. Camprubi E, Jordan SF, Vasiliadou R, Lane N. Iron catalysis at the origin of life. *IUBMB Life.* 2017; 69:373–381. [PubMed: 28470848]
25. Moore EK, Jelen BI, Giovanelli D, Raanan H, Falkowski PG. Metal availability and the expanding network of microbial metabolisms in the Archaean eon. *Nat Geosci.* 2017; 10:629–636.
26. Guan G, et al. Reduction of aqueous CO₂ at ambient temperature using zero-valent iron-based composites. *Green Chemistry.* 2003; 5:630–634.
27. Boekhoven J, Hendriksen WE, Koper GJM, Eelkema R, van Esch JH. Transient assembly of active materials fueled by a chemical reaction. *Science.* 2015; 349:1075–1079. [PubMed: 26339025]
28. Evans MCW, Buchanan BB, Arnon DI. A new ferredoxindependent carbon reduction cycle in a photosynthetic bacterium. *Proc Natl Acad Sci USA.* 1966; 55:928–934. [PubMed: 5219700]
29. Wächtershauser G. Before enzymes and templates: theory of surface metabolism. *Microbiol Rev.* 1988; 52:452–484. [PubMed: 3070320]
30. Smith, E., Morowitz, HJ. *The Origin and Nature of Life on Earth: The Emergence of the Fourth Geosphere.* Cambridge Univ Press; Cambridge: 2016.
31. Morowitz HJ, Kostelnik JD, Yang J, Cody GD. The origin of intermediary metabolism. *Proc Natl Acad Sci USA.* 2000; 97:7704–7708. [PubMed: 10859347]
32. Smith E, Morowitz HJ. Universality in intermediary metabolism. *Proc Natl Acad Sci USA.* 2004; 101:13168–13173. [PubMed: 15340153]
33. Braakman R, Smith E. The emergence and early evolution of biological carbon-fixation. *PLoS Comp Biol.* 2012; 8:e1002455.
34. Braakman R, Smith E. The compositional and evolutionary logic of metabolism. *Phys Biol.* 2013; 10:011001. [PubMed: 23234798]
35. Chandra, et al. The abiotic chemistry of thiolated acetate derivatives and the origin of life. *Sci Rep.* 2016; 6:29883. [PubMed: 27443234]
36. Roldan A, et al. Bio-inspired CO₂ conversion by iron sulfide catalysts under sustainable conditions. *Chem Commun.* 2015; 51:7501–7504.
37. Klöck W, Palme H, Tobschall HJ. Trace elements in natural metallic iron from Disko Island Greenland. *Contributions to Mineralogy and Petrology.* 1986; 93:273–282.
38. McCollom TM. Abiotic methane formation during experimental serpentinization of olivine. *Proc Natl Acad Sci USA.* 2016; 113:13965–13970. [PubMed: 27821742]

39. Sleep NH, Meibom A, Fridriksson Th, Coleman RG, Bird DK. H₂-rich fluids from serpentization: geochemical and biotic implications. *Proc Natl Acad Sci USA*. 2004; 101:12818–12823. [PubMed: 15326313]
40. Frost DJ, et al. Experimental evidence for the existence of iron-rich metal in the Earth's lower mantle. *Nature*. 2004; 428:409–412. [PubMed: 15042086]
41. Darling, DJ. *The Universal Book of Astronomy*. Vol. 260. Wiley; Hoboken, NJ: 2004.
42. Krot AN, Keil K, Scott ERD, Goodrich CA, Weisberg MK. *Treatise on Geochemistry* (second edition). 2014; 1:1–63.
43. Russell, MJ., Hall, AJ., Mellersh, AR. *Natural and Laboratory Simulated Thermal Geochemical Processes*. Springer; Netherlands, Dordrecht: 2003. p. 325-388.
44. Bassez M-P. Water, air, earth and cosmic radiation. *Orig Life Evol Biosph*. 2015; 45:5–13.
45. Bassez M-P. Anoxic and oxic oxidation of rocks containing Fe(II)Mg-silicates and Fe(II)-monosulfides as source of Fe(III)-minerals and hydrogen. *Geobiotropy. Orig Life Evol Biosph*. 2017; 47:453–480. [PubMed: 28361301]
46. Cooper G, Reed C, Nguyen D, Carter M, Wang Y. Detection and formation scenario of citric acid, pyruvic acid, and other possible metabolism precursors in carbonaceous meteorites. *Proc Natl Acad Sci USA*. 2011; 108:14015–14020. [PubMed: 21825143]
47. Orgel LE. The implausibility of metabolic cycles on the prebiotic earth. *PLoS Biol*. 2008; 6:e18. [PubMed: 18215113]

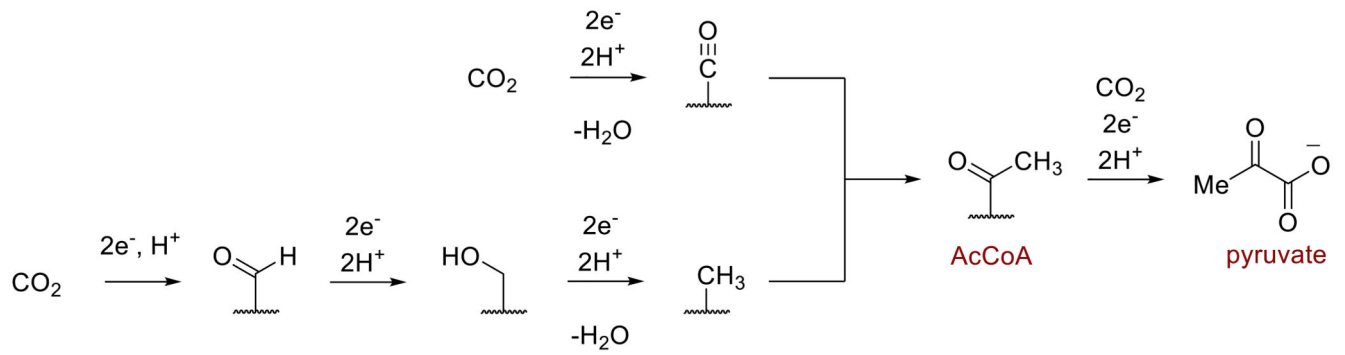


Fig. 1. Mechanistic outline of the ATP-independent AcCoA pathway found in archaea. The reductive carboxylation of AcCoA to pyruvate is also found in the first step of the rTCA cycle. For clarity, organic and metallic co-factors are depicted as a squiggly line.

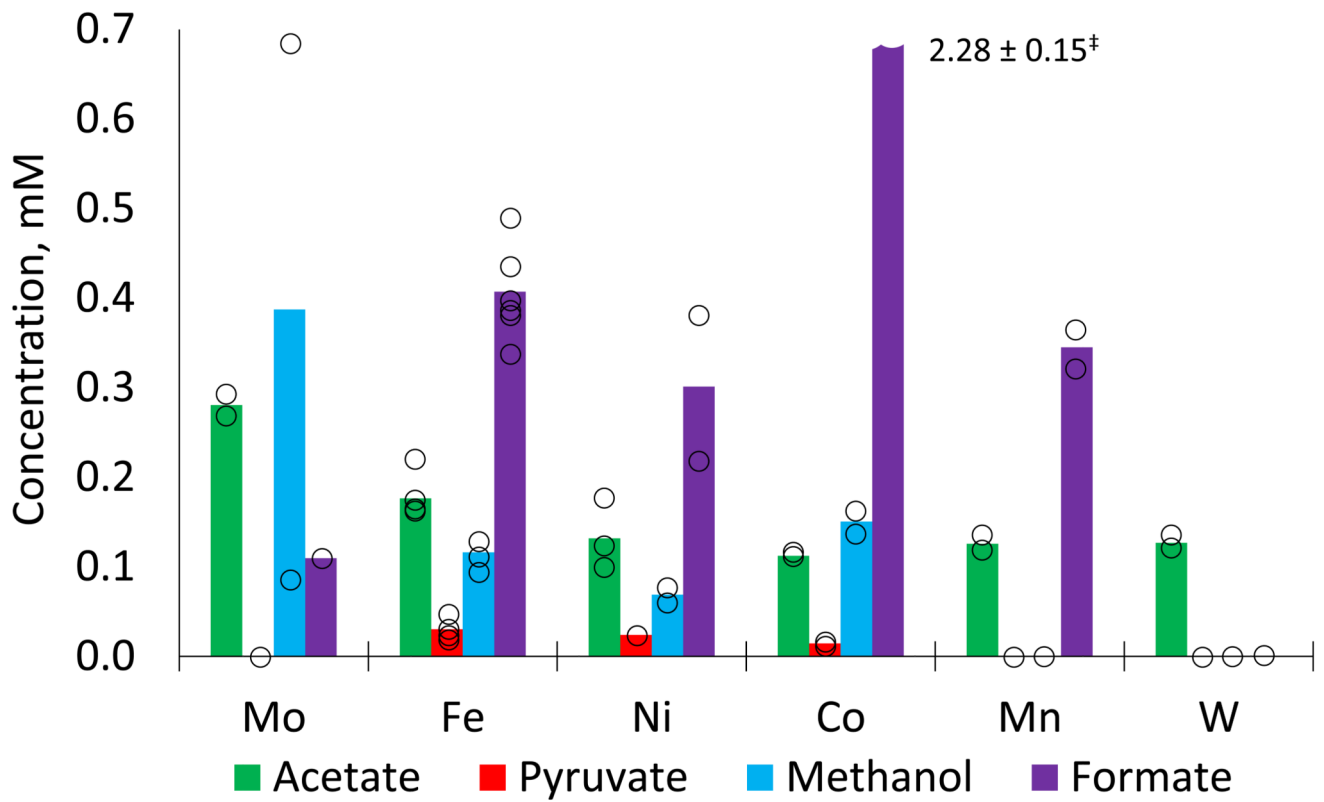
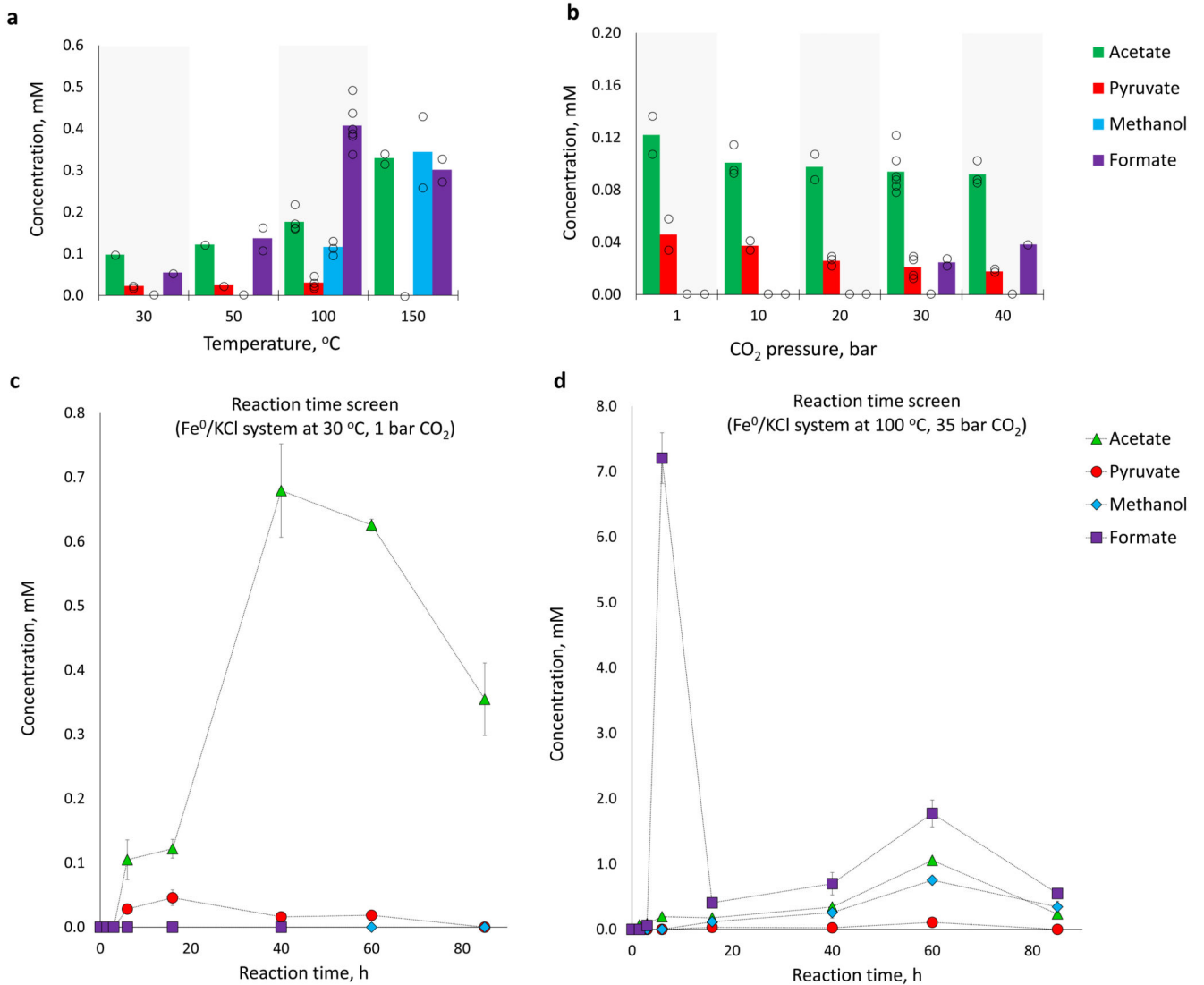


Fig. 2.

Carbon fixation by metals under hydrothermal conditions: 100 °C, 35 bar CO₂, 1 M KCl in H₂O, pH = 7 (except for Mo, where the initial unbuffered pH was 2), 16 h (see SI for experimental and analytical details, as well as error analysis). Bar chart shows mean values of at least two independent runs. ‡ Formate concentrations: 2.13 mM, 2.44 mM; reported error corresponds to mean standard deviation.

**Fig. 3.**

Effect of temperature, pressure and reaction time on iron-promoted CO₂ fixation in aqueous solution. **a** Effect of temperature (35 bar CO₂; 16 h). **b** Effect of CO₂ pressure (30 °C; 16 h). **c** Reaction progress over time (30 °C; 1 bar CO₂). **d** Reaction progress over time (100 °C; 35 bar CO₂). All reactions are 1 M Fe in 1 mL of a 1 M KCl solution. In **a** and **b** bar charts show mean values of at least two independent runs. In **c** and **d** error bars correspond to the mean average deviation from at least two independent runs. Lines connecting the data points do not represent a model fit.

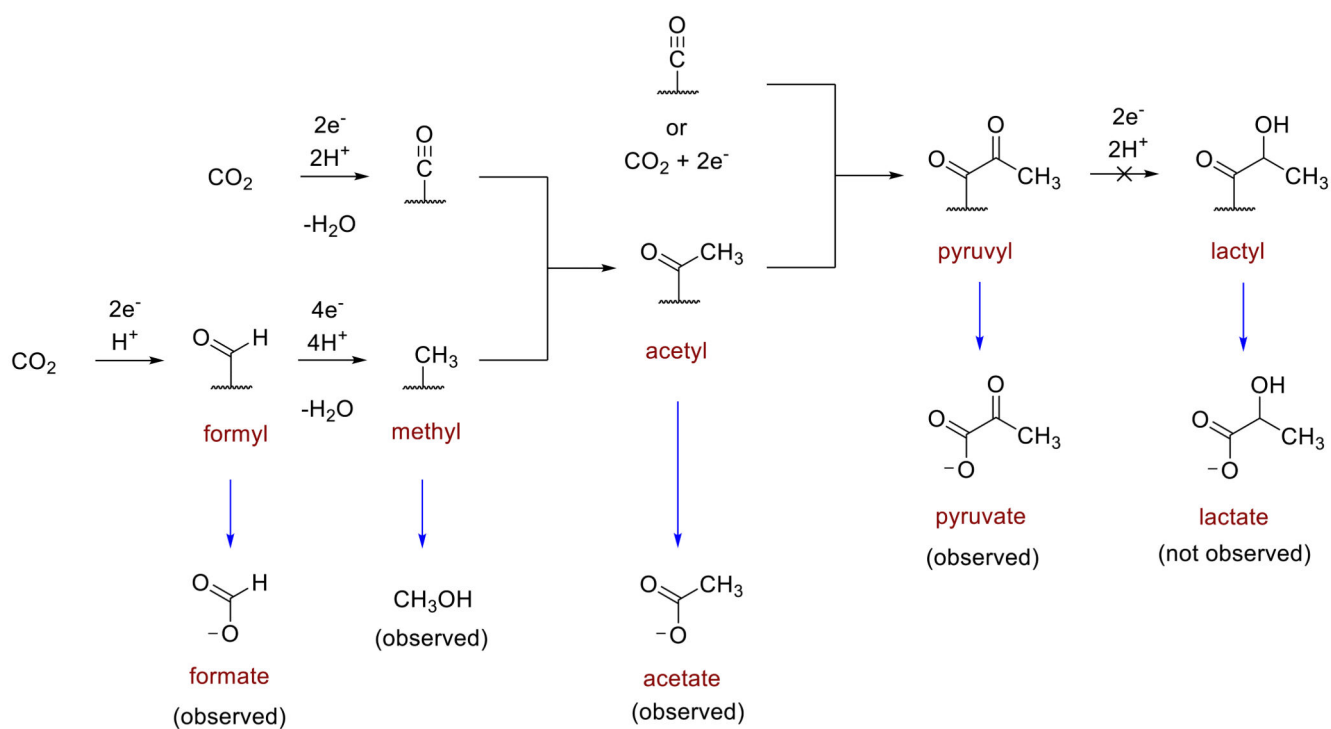


Fig. 4. Plausible mechanism for carbon fixation on the surface of Fe⁰ accounting for the detection of formate, methanol, acetate and pyruvate in aqueous solution upon hydrolysis with KOH. The depicted surface bound acyl structures are deliberately ambiguous and may represent a surface-bound carboxylate or an acyl metal species.

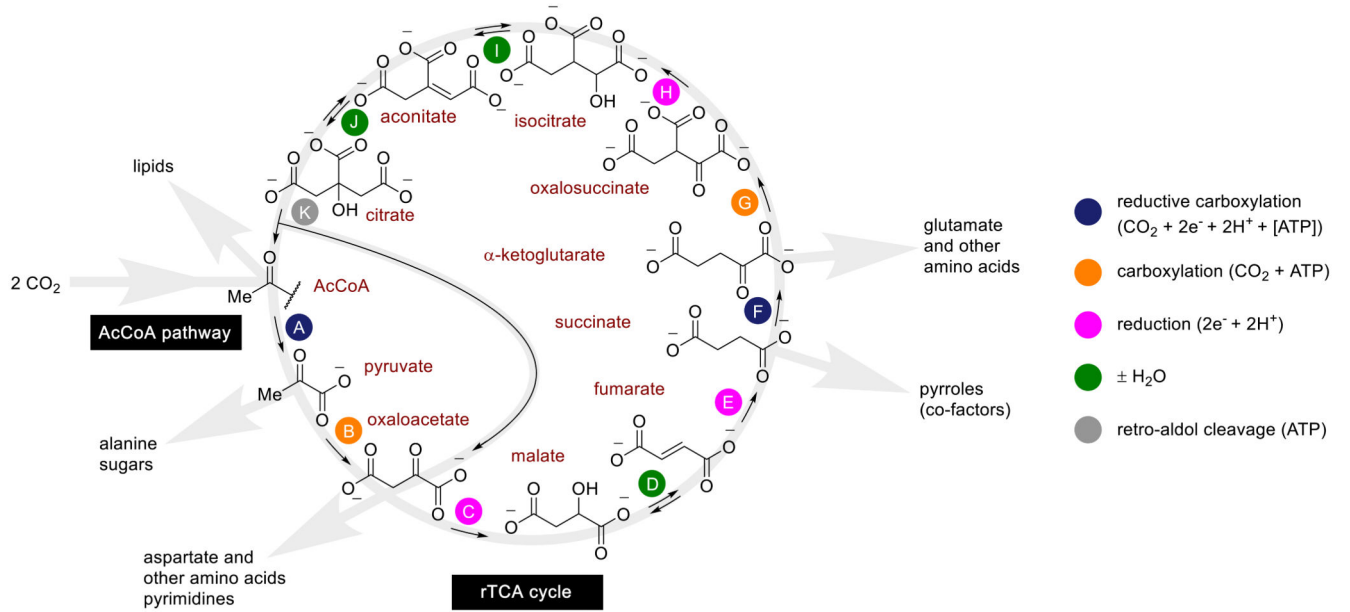


Fig. 5. Hypothetical ancestral proto-anabolic network consisting of a hybrid of the AcCoA pathway and the rTCA cycle, showing the role of its intermediates as universal biosynthetic precursors. The 11 steps of the cycle (A-K) have been assigned colour-coded labels according to their chemical mechanism.